Journal of Materials Chemistry B

PAPER

View Article Online
View Journal | View Issue

Cite this: J. Mater. Chem. B, 2014, 2, 1576

Photostable BODIPY-based molecule with simultaneous type I and type II photosensitization for selective photodynamic cancer therapy†

Yen-Chih Lai and Cheng-Chung Chang*

Received 1st November 2013
Accepted 19th December 2013

DOI: 10.1039/c3tb21547d

www.rsc.org/MaterialsB

We introduce a new class of photostable, efficient photosensitizers based on boron-dipyrromethene (BODIPY) derivatives that can generate singlet oxygen and superoxide simultaneously under irradiation. First, we report the synthesis and design of how to control the generation of a specifically substituted position of BODIPY. Second, after biologically evaluating the uptake, localization and phototoxicity in cell lines, we conclude that 2,6-di-anisole substituted BODIPY is a potentially selective photodynamic therapy candidate because its photodamage is more efficient in cancer cells than in normal cells without significant dark toxicity.

1. Introduction

Photodynamic therapy (PDT) involves the uptake of a photosensitizer by cancerous tissues or other sites of the therapeutic target, followed by selective irradiation with visible or near IR light of an appropriate wavelength that is absorbed by the photosensitizer. There are three fundamental requirements for PDT that are oxygen, a light source, and a photosensitizer. Each factor is harmless by itself, but their combination can produce cytotoxic agents.[1–3] There are many reported or commercially available photosensitizers. By comparison, cyclic tetrapyrroles (porphyrins, chlorins, and bacteriochlorins) are difficult to synthesize and modify; while phenothiazinium-based structures might be made more easily but present low light-to-dark toxicity ratios.[4–6] Most photosensitizers present application limitations, such as a low photostability, structural instability, or usable range of solvent conditions.[7] Thus, it is important to develop a new generation of photosensitizers with high efficiency and photostability that are widely applicable in various conditions.

Selective photodamage is the most important criterion for a superior PDT reagent. The efficient delivery of a photosensitizer to cancer cells and its subcellular distribution not only depend on cellular processes but also on the physicochemical properties and structural characteristics of the molecule itself.[8] Therefore, several strategies have been developed to improve the selective delivery of sensitizers to tumour tissues, including their conjugation to carrier proteins,[9] oligonucleotides,[10] monoclonal antibodies,[11] epidermal growth factors,[12] carbohydrates,[13] and hydrophilic polymers.[14] However, these high molecular weight branched-peptide conjugates are difficult to synthesize, purify, and characterize. Although enhanced cellular uptake and selectivity for tumour tissues have been achieved with some porphyrin sensitizers, most of these are usually found in cytoplasmic membranes rather than in sensitive intracellular sites, such as the mitochondria, the endoplasmic reticulum (ER), and the nuclei.

BODIPY (boron-dipyrromethene) derivatives offer large absorption extinction coefficients, sharp fluorescence emissions with high fluorescence quantum yields, photostability and low sensitivity to environmental variation.[15] Thus, BODIPY derivatives have attracted much research interest and have been used for many applications.[16] The new application of BODIPY derivatives for photosensitizers was achieved by attaching a functional group which can offer electrons to stabilize that photoexcited BODIPY core and to quench the emission from the singlet state, thereby promoting a triplet state lifetime.[17] Specifically, heavy atoms are incorporated into the structure as a strategy to facilitate intersystem crossing and to promote the singlet oxygen yield to become a new generation of photosensitizers for photodynamic therapy.[18,19] This appears to satisfy the required criteria for a good photosensitizer (high singlet oxygen yield, photostability and long wavelength absorption); however, this approach disobeys the principle of dark-non-toxicity for a photosensitizer to be a PDT candidate.[20] More importantly, based on the above considerations, it is rare to find BODIPY-based photosensitizers which present selective photodamage to cancer but not normal cells or tissues. Hence, it is possible to design and produce, with appropriate chemical modification, a new generation of BODIPY-based photosensitizers that can overcome the issues of dark-toxicity and

Graduate Institute of Biomedical Engineering, National Chung Hsing University, 250 Kuo Kuang Road, Taichung, 402, Taiwan, ROC. E-mail: ccchang555@dragon.nchu.edu.tw; Fax: +886-4-22852422

† Electronic supplementary information (ESI) available: Synthesis and characterization, Fig. S1 and S2. See DOI: 10.1039/c3tb21547d

nonselective photodamage without losing their unique optical characteristics.

In this study, we report a novel photosensitizer that is highly efficient, photostable, and more importantly, showed selective PDT behaviour. This strategy can be easily achieved by attaching an aryl group directly onto the pyrrole moiety of BODIPY, but this is not more expensive than dimethyl pyrrole. By controlling the bromination sequence, 3,5- or 2,6-diaryl substituted BODIPY derivatives can be collected with good yield. Preliminary biological studies on one of these dyes indicate that this type of compound is highly membrane permeable, and it can selectively localize within specific subcellular organelles, suggesting promising PDT applications for these molecules.

2. Experimental

2.1 Materials

The general chemicals employed in this study were the highest grade available and were obtained from Acros Organic Co., Merck Ltd., or Aldrich Chemical Co. and used without further purification. All of the solvents were of spectrometric grade.

2.2 Apparatus

The absorption spectra were generated using a Thermo Genesys 6 UV-visible spectrophotometer, and the fluorescence spectra were recorded using a HORIBA JOBIN-YVON Fluoromas-4 spectrofluorometer with a 1 nm band-pass and a 1 cm cell length at room temperature. The cellular fluorescence images and dual staining fluorescence images were obtained using a Leica AF6000 fluorescence microscope with a DFC310 FX Digital colour camera and a Leica TCS SP5 confocal fluorescence microscope. Fluorescence photographs were taken through the related wavelength ranges using photomultiplier tubes (PMT). The light source used to measure the singlet oxygen yield and PDT cell death was a Xenon Light Source LAX-Cute (Asahi Spectra).

2.3 Cell culture conditions and compound incubation

Human embryonal lung MRC-5 normal fibroblast cells and HeLa human cervical cancer cells were maintained in Modified Eagle's Medium (MEM) containing non-essential amino acids, Earle's salts, L-glutamine, 1 mM sodium bicarbonate, 1 mM sodium pyruvate, 1% (penicillin + streptomycin) and 10% fetal bovine serum (FBS); the human lung adenocarcinoma cell line A549 was maintained in RPMI-1640 medium containing 1% (penicillin + streptomycin), sodium bicarbonate (2.0 g L^{-1}) and 10% FBS. The cells were cultured at 37 °C in a humid atmosphere with 95% air and 5% CO_2. Before the observation of cellular localization, cells were seeded onto coverslips and incubated for 24 h. The next day, cells were incubated with different concentrations of compounds for 12 h, for which the DMSO stock solutions were diluted in serum-free medium before use (1/100 v/v).

2.4 Light-induced cytotoxicity assay

Three different cell types were examined in the assay: the human lung MRC-5 normal cells, lung A549 cancer cells and human cervical HeLa cancer cells. Varying concentrations of compounds were incubated with the cells in the dark for 12 h. Subsequently, the culture medium was removed, and fresh culture medium was added to each well. The plates were irradiated using a light source that is described in the next section and then incubated for a further 24 h at 37 °C. All assay experiments were carried out in triplicate, and an average of the three individual runs are presented. Methylene blue and Foscan were used as comparative standard controls and were assayed according to previously documented procedures.[21]

2.5 Extraction and quantification of compounds in cells

HeLa cells (2×10^6) were seeded into 60 mm × 15 mm cell culture dishes. Before the cells reached ~100% confluence, a compound was added to one dish and incubated for 12 h. For the dishes that were nearly 100% confluent, the conjugate solution was added and incubated from 15 min to 4 h. After incubation with the conjugates, all dishes were washed with PBS. The cells were removed from the substrate with trypsin and then pelleted. The cell suspension was sonicated for 1 h, and 1.8 mL of ethyl acetate was added to each tube to extract the compound. Both absorbance and fluorescence in the organic phase were recorded.

2.6 Measurement

The light source for the measurement of singlet oxygen yield and PDT cell death was a white light (a 20 W xenon lamp that passes through a 400–700 nm mirror module). Before the light was output from the optional light guide and collimator lens, the light passed through a 510 nm long pass (lp) filter (the light power was 6 mW cm^{-2} on the dish surface). The singlet oxygen quantum yields from compounds that were in an organic solvent were determined by a photo-steady-state method using 1,3-diphenylisobenzofuran (DPBF) as the scavenger. Finally, the following equation was utilized to calculate the singlet oxygen quantum yields (Φ_Δ):

$$\Phi_\Delta = [(v/v_{MB}) \times (A_{MB}/A)] \times \Phi_{\Delta,MB}$$

where v is the DPBF oxidation rate, A, the area of absorbance maxima of the compound and MB means methylene blue. The value of singlet oxygen quantum yield (Φ_Δ) for MB is 0.52 in several media and measured with different techniques.[22,23] The superoxide generation from compounds that were in an aqueous solution was determined by a photo-steady-state method using 4-((9-acridinecarbonyl)amino)-2,2,6,6-tetramethylpiperidin-1-oxyl (TEMPO-9-ac, Invitrogen, Carlsbad, CA) as the radical detector. Dual staining of tracker and compound: the cells were first incubated with a compound for 12 h, which was followed by incubation with 5 μM organelle probes (Mito Tracker Green FM for 20 min at 37 °C, ER Tracker™ Green for 30 min at 37 °C), and then washed with PBS before observation. The excitation source was a green light cube, in which the light passed

through a 535 ± 25 nm band pass (bp) filter and the emission was collected through a 590 nm long pass (lp) filter (red emission of compound) and a blue light cube, in which light passed through a 470 ± 20 nm bp filter and the emission was collected through a 510 nm lp filter to collect green emission of probes. Once the definite yellow color image was presented, we said that the compound was co-localized with the probes. PDT-induced phototoxicity was determined using Hoechst 33342 (H-1399, Invitrogen, USA) and propidium iodide (PI, P3566, Invitrogen, USA) under a fluorescence microscope and confirmed by a trypan blue exclusion and staining assay. Determination of quantum yields is relative to Rhodamine B.[24]

3. Results and discussion

3.1 Molecular preparation and basic spectroscopic properties

BODIPY derivatives **2,6-DAB** and **3,5-DAB** were synthesized by following different routes as outlined in Scheme 1. Bromination is the key reaction of molecule preparation in this study. The 8-(4-methoxyphenyl) boron-dipyrromethane, an intermediate precursor of compound **2,6-A**, was obtained upon $BF_3 \cdot Et_2O$ complexation of compound **1**. Then, the 2,6-dibromo substituted BODIPY can be prepared by treating one equivalent of 8-(4-methoxyphenyl) boron-dipyrromethane with 2.2 equivalents of *N*-bromosuccinimide (NBS). Alternatively, when compound **1** was brominated with NBS first, the main product was 3,5-dibromo substituted dipyrromethane, which is unstable because it is easily protonated, especially in the column flushing purification process. That is why we prepared compound **3,5-A** in a sequence of steps in a one pot reaction directly from compound **1** to **3,5-A**. Notably, the use of 2.2 equivalents of NBS provided dibromo-BODIPY in good yield along with a minor amount of mono-substituted bromine. Here we claim that even with an excess amount of the brominating agent, no regioisomeric products, such as 3,5-dibromo-substituted product in **2,6-A** or 2,6-dibromo-substituted product in **3,5-A**, were detected in the reactions. Additionally, in the last step, compounds **2,6-A** and **3,5-A** were both coupled with compound **2** with similar yield in the same reaction conditions. Recently, most literature presented the molecular constructions of unitary 3,5- or 2,6-disubstituted BODIPY were based on dimethylpyrrole coupling with the Wittig reaction. Here we want to emphasize that we can collect the 3,5-disubstituted and 2,6-disubstituted BODIPY products, by using pyrrole as the starting material instead of more expensive dimethylpyrrole. This breakthrough result can be widely applied to organic synthesis.

In this investigation, the BODIPY moiety was selected as the electron acceptor and anisole was chosen as the electron-donating unit. The basic spectral properties in Fig. 1 show that no significant solvent polarity-dependent spectral shifts in the absorption and emission spectra were observed for the two compounds **2,6-DAB** and **3,5-DAB**. However, when comparing the spectral properties of these chromophores, 2,6-disubstituted product **2,6-DAB** showed lower transition energy in all investigated solvents with broader peak patterns in absorption or emission spectra. Meanwhile, higher extinction coefficient values but lower quantum yields were obtained. This finding indicates that, in the ground states, these chromophores are significantly stabilized by solvation and the auxiliary electron-donating ability of anisole units offered better effective

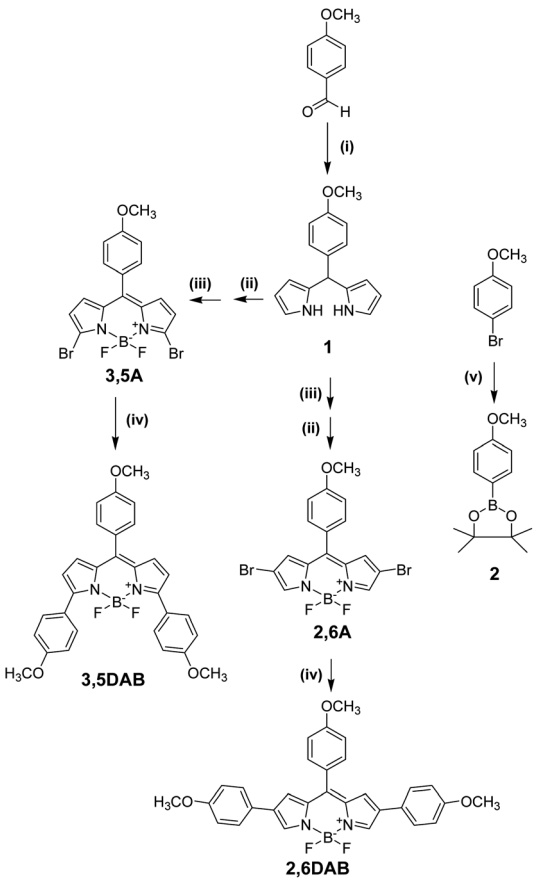

Scheme 1 Synthetic route to BODIPY-based photosensitizers **2,6-DAB** and **3,5-DAB**: (i) pyrrole, TFA, rt. (ii) NBS, THF, ice bath. (iii) DDQ, THF, rt. then $Et_3N-BF_3 \cdot OEt_2$, toluene, reflux. (iv) K_2CO_3, (*o*-tol)$_3$P, $Pd(OAc)_2$, DME/H_2O = 5/1, compound **2**, reflux. (v) $Pd(PPh_3)_2Cl_2$, pinacolborane, dioxane/Et_3N, reflux.

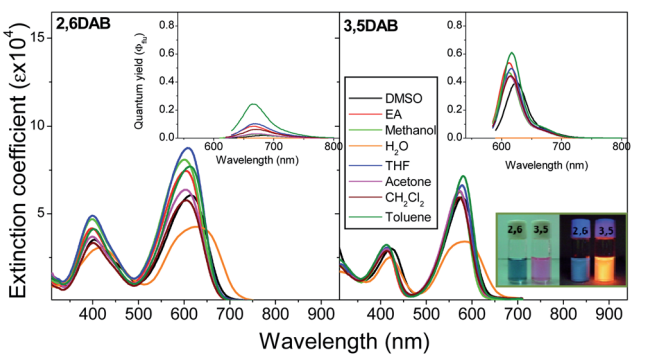

Fig. 1 Absorption (left) and emission (right) spectra of compound **2,6-DAB** (left) and **3,5-DAB** (right) in different solvents; characterized by extinction coefficient and quantum yield, respectively. Excited wavelengths are depicted as absorption maxima.

conjugation to the BODIPY core. However, 3,5-disubstituted product compound **3,5-DAB** exhibited more stable absorption and luminescence properties in most organic solvents, especially with quantum yields ranging from 0.4 to 0.6. Based on our knowledge, fluorophores that can be successfully applied were based on a single type of fluorophore structure, common to all integrated sensor molecules. The fluorescent optical property of **3,5-DAB** makes this proposal possible once we design and synthesize derivatives with suitable spacers or functional groups, so that it becomes 3,5-dialkoxyphenyl substituted BODIPY, which will be applied in optical sensors, non-doped OLEDS, or laser dyes. Furthermore, we expect that this type of fluorophore will be useful as a cellular probe because of its unique optical property.

3.2 Singlet oxygen generation and photostability

The singlet-oxygen production study was undertaken by monitoring the reaction of the known singlet oxygen acceptor 1,3-diphenylisobenzofuran (DPBF) with photosensitizer-generated singlet oxygen.[25] This production was achieved experimentally by following the disappearance of the 410 nm absorbance band of DPBF at an initial concentration of 20 μM (2 fold the concentration of the compound). The rates of DPBF oxidation by these two compounds in DMSO solvent were investigated by exciting the absorptions of the compounds (Fig. 2). When placed under the white light source (400–700 nm, no filter) or visible light source (400–700 nm with a 510 nm long pass filter) for the irradiation period, compound **2,6-DAB** presented a slightly better DPBF oxidation rate than compound **3,5-DAB**. Based on the result of Fig. 2, the estimated singlet oxygen yields were about equal to the level of methylene blue (MB). Here, as described in the Experimental, the singlet oxygen quantum yields (Φ_Δ) of compound **2,6-DAB** and **3,5-DAB** were obtained as 0.48 and 0.53 by the relative method using methylene blue as the reference ($\Phi_\Delta = 0.52$). However, the singlet oxygen generations apparently increase when the system was irradiated under a white light source. This finding indicates that the S_0–S_2 transition absorption bands of the compound at approximately 400 nm contribute some singlet oxygen yield. Additionally, the inset in Fig. 2b shows that under this irradiation condition, the photostabilities of compounds are better than MB. It is known that good photostability upon repetitive excitation is highly desirable in PDT application because photobleaching of photosensitizers usually produces photodegradation side products that may lower the efficiency of reactive oxygen species (ROS) generation. Moreover, when a photosensitizer is used as a tumour-visualizing tool in PDT, high photostability is required to allow monitoring for a sufficiently long period.[26]

3.3 Real-time photodamage and photostability in cells

Once these two compounds presented the characteristic behaviours of singlet oxygen generation and photostability, we examined whether the compounds can be used as a tool for cell photosensitization. Fig. 3 illustrates the photodamage process from a real-time video recorded under a fluorescence microscope with a colour CCD. This distinction was revealed by the

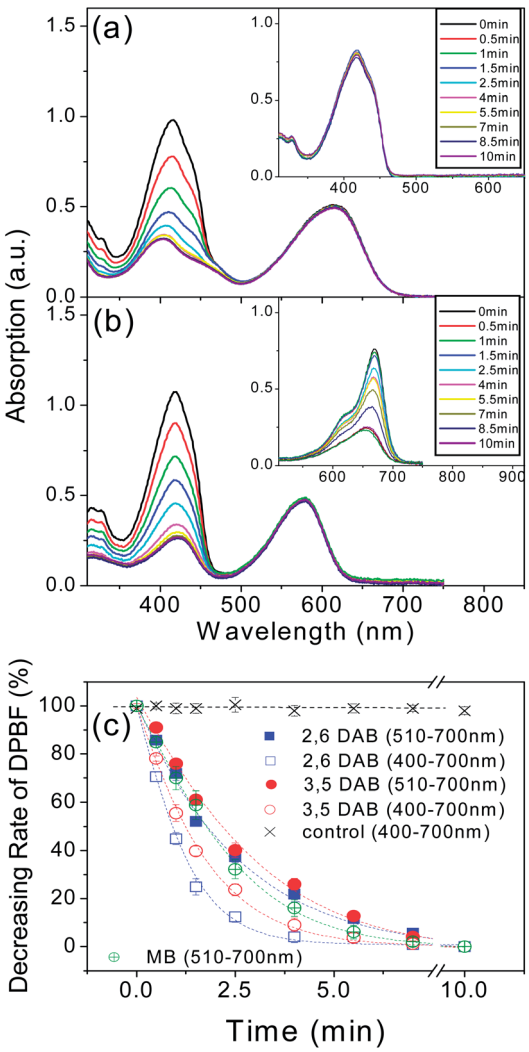

Fig. 2 Absorption spectra variations of 20 μM DPBF consumption in the presence of 10 μM (a) **2,6-DAB** and (b) **3,5-DAB** in DMSO after irradiation with an average 6 mW cm^{-2} for the 510 nm lp through the filter. Relative DPBF oxidation rates by singlet oxygen, which were generated from the compounds, are plotted in (c); the data without the 510 nm lp filter are also shown. Each data point represents the average from three separate experiments. (Inset: (a) control DPBF without adding a compound, (b) identical experimental condition but with methylene blue (MB).)

system measured fluorescence using a 535 ± 25 nm band pass filter as an exciting light source and collected through a red filter (590 nm long pass). It is clear that plasma membrane bleb formation and acute cell death were caused by illumination with green light for cells that were incubated with a compound. Here, irradiated time dependent fluorescent images show nearly constant emission intensities, which further confirms the photostability behaviour in Fig. 2; these two compounds both cause apparent photodamage to cancer cells, but only compound **2,6-DAB** presents little or no collateral damage to normal cells. Here, the important message is that in our studied system, 2,6-disubstituted BODIPY (**2,6-DAB**) possibly shows selective PDT to cancer cells rather than 3,5-disubstituted BODIPY (**3,5-DAB**), even in unclear fluorescent images because

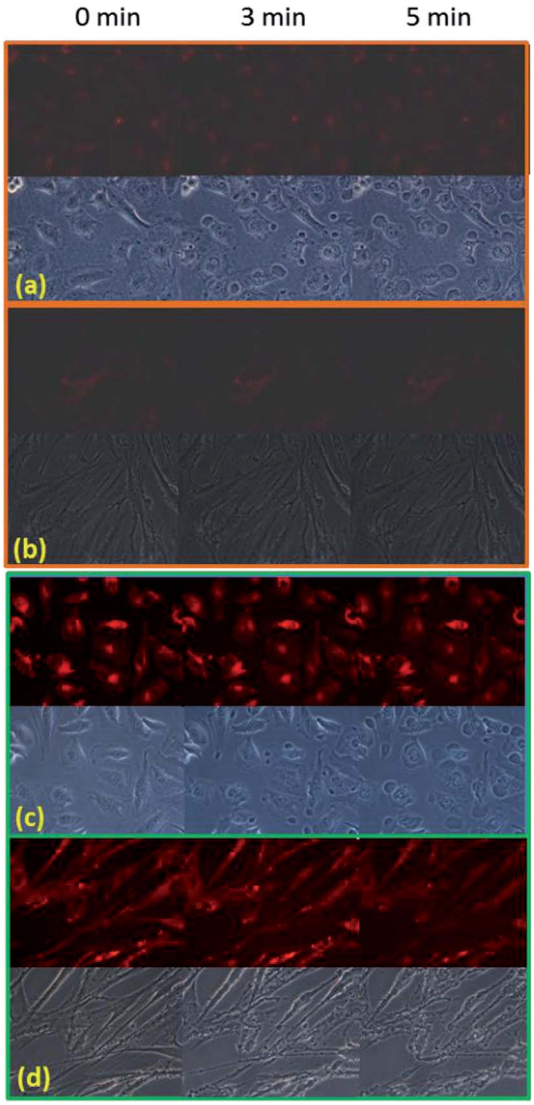

Fig. 3 Several selected fluorescent and bright-field photodamage images from a real-time video of (a and c) HeLa cancer cells, and (b and d) MRC-5 normal cells incubated with 10 μM **2,6-DAB** (a and b) or **3,5-DAB** (c and d) for 12 h after 535 ± 25 nm irradiation from a mercury lamp for fluorescent microscopy.

of low quantum yield. This result suggests that **2,6-DAB** is a potentially useful reagent for cell photosensitization, studies on oxidative stress, or PDT.

3.4 Intracellular accumulation

Following the experimental conditions of Fig. 3, we tried to determine the quantitative accumulation of compounds in the cells using red (590 nm long pass) filters, as in Fig. S1.† The compound **3,5-DAB** presented clearer concentration-dependent intracellular fluorescent signals because of the compound's higher emission quantum yield, and these intracellular accumulation images appear no different between cancer cells and normal cells. The intracellular accumulation of compound **2,6-DAB** is difficult to observe because of its low fluorescent quantum yield. Thus, the kinetics of compound uptake was determined by the extraction of the compound from cells.[27] By monitoring the absorbance and fluorescence intensities of compounds in the ethyl acetate layer after extracting from the cells, as in the Experimental section description, the increase in the compound concentration in the cells was quantified (Fig. 4). It is clearly confirmed that the cellular uptake of **3,5-DAB** appears no different between cancer and normal cells, whereas **2,6-DAB** accumulated in the cancer cells more than in the normal cells. This notable observation supports us to propose that the uptake difference between cancer and normal cells is the dominant factor for selective photodamage.

3.5 Sub-cellular localization

It is known that the intracellular localization of photosensitizers strongly affects the mechanism of cell death. The biological efficacy for most photodynamic therapy (PDT) sensitizers of tumors depends on their efficient translocation across cellular membranes and their delivery into specific organelles within cancer cells.[28] To determine the localization of each compound, as detailed in the Experimental section, the cells incubated with compound **2,6-DAB** were double stained with cellular tracker green, which merged with the red light emission region of the compound. Fig. 5 reveals that **2,6-DAB** is

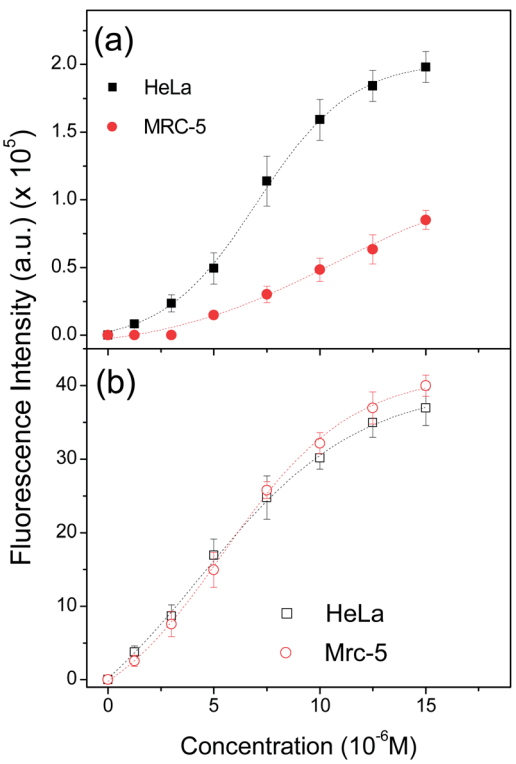

Fig. 4 Intracellular accumulations of **2,6-DAB** (a) and **3,5-DAB** (b) in normal (MRC-5) and cancer (HeLa) cells. The cells were incubated with variable concentrations of compounds for 12 h, and the intracellular uptake was determined from a fluorescence calibration curve of the ethyl acetate layer after extracting from the cells. Each data point represents the average from three separate experiments.

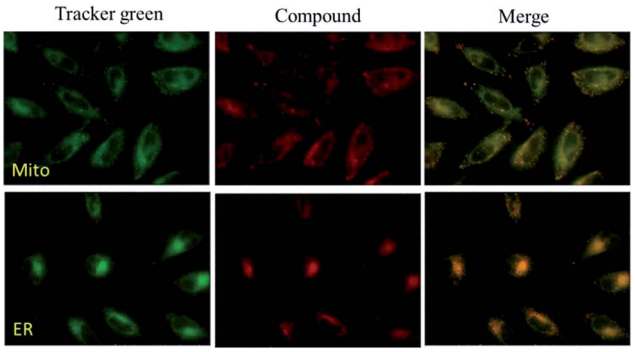

Fig. 5 Sub-cellular localization of **2,6-DAB** in HeLa cancer cells: the images of tracker green were excited by a blue light cube that passed light through a 470 ± 20 nm bp filter, and emission was collected through a 510 nm lp filter. The red images of the compound were excited by a green light cube that passed light through a 535 ± 25 nm bp filter, and emission was collected through a 590 nm lp filter.

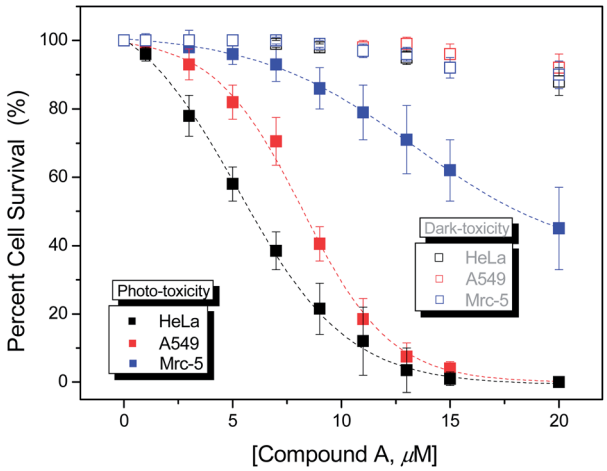

Fig. 6 Phototoxicity of cells treated with variable concentrations of **2,6-DAB** for 12 h before irradiation and irradiated with a 510 nm lp light source (average 8 J cm^{-2}); cell death was tested overnight. Each data point represents the average from three separate experiments and the irradiation condition details are described in the Experimental section.

localized predominantly in the endoplasmic reticulum (ER) and less in the mitochondria of cancer cells.

Generally, mitochondrial photodamage has been reported to be the primary cause of apoptosis during PDT because the mitochondria play an integral role in various cell biological processes, such as energy production, apoptotic cell death, molecular metabolism, calcium signaling, and cell redox status.[29–31] However, ER is also a very attractive site for the localization of the photosensitizers to improve the efficiency of PDT. It is known that oxidation of ER proteins due to PDT may cause changes in ER Ca^{2+} homeostasis and/or aggregation of unfolded and misfolded proteins.[32] For example, the ER-localizing photosensitizer Foscan was recently shown to cause Bcl-2 photodamage, possibly specifically affecting the ER pool of Bcl-2 in cancer cells.[33,34] Based on the literature, PDT with photosensitizers that target mitochondria and ER will very possibly cause photodamage to Bcl-2 and Bcl-Xl,[35] and this type of photodamage to these antiapoptotic proteins is observed immediately upon light exposure,[36] as in Fig. 3. It is doubtless that the ability of PDT to affect Bcl-2 function plays a crucial role in tumour treatment.

3.6 Phototoxicity

The combination of compound **2,6-DAB** and light illumination resulted in quantitative cellular toxicity. Fig. 6 reveals that three different cell lines displayed no determinable dark toxicity with **2,6-DAB** up to a concentration of 15 μM. By contrast, irradiation with 8 J cm^{-2} of 510 nm long pass light dose showed a significant light-induced toxicity with EC50 values determined for HeLa, A549, and MRC-5 as 5.7, 8.2 and 18.5 μM, respectively. A more apparent phototoxicity result was observed when the system was irradiated under white light (400–700 nm) as the PDT light source. On the other hand, an interesting result was observed when the cell death was determined with double staining Hoechst 33342 as well as PI.[37,38] Fig. S2† shows that in the early stage of cell death (two probes stained once immediately after illuminating), fluorescent images result in apparent blue emission enhancement in the nucleus. This result is because of the interaction between Hoechst and condensed DNA. This occurred when the red fluorescence from PI became dominant in the nucleus when the irradiated cell line was cultured overnight. It is likely that the nuclear membrane is damaged during a later period after irradiation. This cell death pathway is likely because of an anti-apoptosis protein of mitochondria or ER, as discussed above. However, we provided an additional PDT reagent as another choice, and this is the first report for a BODIPY derivative to show selective PDT to cancer cells but not normal cells.

3.7 New reactive oxygen species generation

It is notable that the PDT effects of **2,6-DAB** are better than we expected. Hence, we examined the possibility for this compound's PDT progress by other possible mechanisms, such as type I PDT. The type I mechanism involves hydrogen-atom abstraction or electron-transfer between the excited sensitizer and a substrate, yielding free radicals. These radicals can react with oxygen to form an active oxygen species, such as the superoxide radical anion.[39,40] Most studies generally infer that singlet oxygen formation of type II PDT is primarily responsible for the biological PDT effect; however, several recent studies indicate that radical species from the type I mechanism may lead to an amplified PDT response, particularly under low oxygen conditions.[41,42] It is reported that these two competing mechanisms can occur simultaneously.[28,43] The free radical probe 4-((9-acridinecarbonyl)amino)-2,2,6,6-tetramethylpiperidin-1-oxyl (TEMPO-9-ac, Invitrogen, Carlsbad, CA) captures radicals, resulting in fluorescence turn-on ($\lambda_{ex/em}$ = 358/440 nm).[44] Irradiation of **2,6-DAB** also generated a more apparent increase in signal from TEMPO-9-ac compared to unchanged levels of the control (Fig. 7). This finding indicates that compound **2,6-DAB** may undergo type I and II PDT

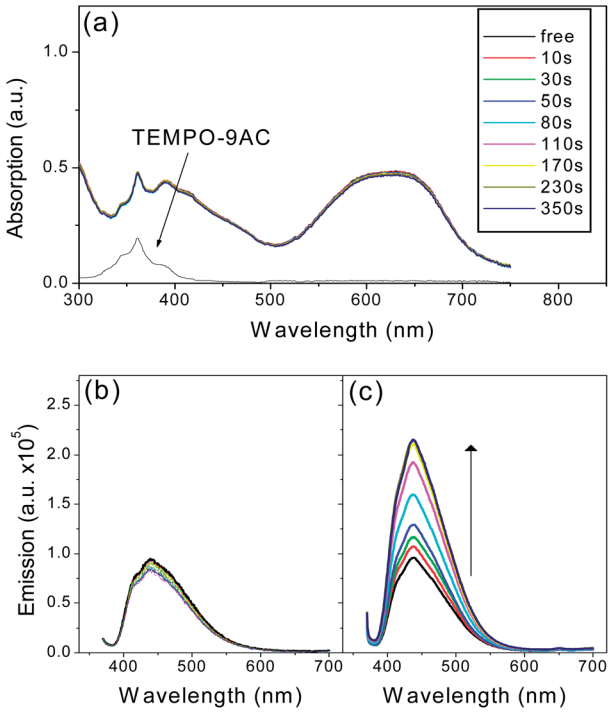

Fig. 7 (a) Absorption spectra of TEMPO-9ac upon irradiation with compound **2,6-DAB**. Experimental conditions follow Fig. 2. Emission (λ_{ex} = 360 nm) spectra of TEMPO-9ac upon irradiation without compound (b) and with compound **2,6-DAB** (c).

simultaneously when it stays in the cells. We proposed that is why the PDT effects of **2,6-DAB** are better than we expected.

4. Conclusions

BODIPY offers many superior optical properties. In this study, we have successfully applied BODIPY derivatives for cancer targeting and demonstrated that the 2,6-di-anisole substituted product **2,6-DAB** may be a potent tumor-specific photosensitizer for PDT. First, we presented a cheap and convenient synthesis procedure that can be widely applied to prepare diversified BODIPY derivatives. Second, ROS generation as well as biological evolution of cellular uptake, localization and phototoxicity was determined. Therefore, the PDT characteristics of the **2,6-DAB** compound include (1) target selectivity for the PDT of cancer cells; (2) higher photostability than methylene blue; (3) supported extra phototoxicity with superoxide generation.

Acknowledgements

This work was supported financially by the National Science Council (NSC 101-2113-M-005-016-MY3) of Taiwan.

Notes and references

1 J. C. Kennedy, R. H. Pottier and D. C. Pross, *J. Photochem. Photobiol., B*, 1990, **6**, 143–148.
2 J. D. Spikes, *Ann. N. Y. Acad. Sci.*, 1975, **244**, 496–508.
3 M. Ochsner, *J. Photochem. Photobiol., B*, 1997, **39**, 1–18.
4 E. S. Nyman and P. H. Hynninen, *J. Photochem. Photobiol., B*, 2004, **73**, 1–28.
5 M. Wainwright, *Photodiagn. Photodyn. Ther.*, 2005, **2**, 263–272.
6 M. Wainwright, D. A. Phoenix, L. Rice, S. M. Burrow and J. Waring, *J. Photochem. Photobiol., B*, 1997, **40**, 233–239.
7 E. A. Lissi, M. V. Encinas, E. Lemp and M. A. Rubio, *Chem. Rev.*, 1993, **93**, 699–723.
8 D. Kessel, *J. Porphyrins Phthalocyanines*, 2004, **8**, 1009–1014.
9 M. R. Hamblin and E. L. Newman, *J. Photochem. Photobiol., B*, 1994, **26**, 147–157.
10 B. Mestre, M. Pitie, C. Loup, C. Claparols, G. Pratviel and B. Meunier, *Nucleic Acids Res.*, 1997, **25**, 1022–1027.
11 R. Hudson, M. Carcenac, K. Smith, L. Madden, O. J. Clarke, A. Pelegrin, J. Greenman and R. W. Boyle, *Br. J. Cancer*, 2005, **92**, 1442–1449.
12 A. Gijsens, L. Missiaen, W. Merlevede and P. de Witte, *Cancer Res.*, 2000, **60**, 2197–2202.
13 G. Li, S. K. Pandey, A. Graham, M. P. Dobhal, R. Mehta, Y. Chen, A. Gryshuk, K. Rittenhouse-Olson, A. Oseroff and R. K. Pandey, *J. Org. Chem.*, 2004, **69**, 158–172.
14 M. Tijerina, P. Kopeckova and J. Kopecek, *Pharm. Res.*, 2003, **20**, 728–737.
15 A. Loudet and K. Burgess, *Chem. Rev.*, 2007, **107**, 4891–4932.
16 H. Kabayashi, M. Ogawa, R. Alford, P. L. Choylle and Y. Urano, *Chem. Rev.*, 2010, **110**, 2620–2640.
17 A. Kamkaew, S. H. Lim, H. B. Lee, L. V. Kiew, L. Y. Chung and K. Burgess, *Chem. Soc. Rev.*, 2013, **42**, 77–88.
18 N. Adarsh, R. R. Avirah and D. Ramaiah, *Org. Lett.*, 2010, **12**, 5720–5723.
19 T. Yogo, Y. Urano, Y. Ishitsuka, F. Maniwa and T. Nagano, *J. Am. Chem. Soc.*, 2005, **127**, 12162–12163.
20 S. H. Lim, C. Thivierge, P. Nowak-Sliwinska, J. Han, H. van den Bergh, G. Wagnieres, K. Burgess and H. B. Lee, *J. Med. Chem.*, 2010, **53**, 2865–2874.
21 M. H. Teiten, L. Bezdetnaya, P. Morlière, R. Santus and F. Guillemin, *Br. J. Cancer*, 2003, **88**, 146–152.
22 F. Wilkinson, W. P. Helman and A. B. Ross, *J. Phys. Chem. Ref. Data*, 1993, **22**, 113–262.
23 R. W. Redmond and J. N. Gamlin, *Photochem. Photobiol.*, 1999, **70**, 391–475.
24 R. A. Velapoldi and H. H. Tonnesen, *J. Fluoresc.*, 2004, **14**, 465–471.
25 K. Gollnick and A. Griesbeck, *Tetrahedron*, 1985, **41**, 2057–2068.
26 J. Moan, *Cancer Lett.*, 1986, **33**, 45–53.
27 Y. Cheng, A. C. Samia, J. Li, M. E. Kenney, A. Resnick and C. Burda, *Langmuir*, 2010, **26**, 2248–2255.
28 T. J. Dougherty, C. J. Gomer, B. W. Henderson, G. Jori, D. Kessel, M. Korbelik, J. Moan and Q. Peng, *J. Natl. Cancer Inst.*, 1998, **90**, 889–905.
29 A. P. Castano, T. N. Demidova and M. R. Hamblin, *Photodiagn. Photodyn. Ther.*, 2005, **2**, 1–23.
30 N. Dias and C. Bailly, *Biochem. Pharmacol.*, 2005, **70**, 1–12.
31 M. E. Rodriguez, K. Azizuddin, P. Zhang, S. M. Chiu, M. Lam, M. E. Kenney, C. Burda and N. L. Oleinick, *Mitochondrion*, 2008, **8**, 237–246.

32 R. Michael and P. M. Hamblin, *Advances in Photodynamic Therapy: Basic, Translational, and Clinical*, Artech House, Incorporated, 2008, 28.36.37.55.71-74.
33 H. R. Kim, Y. Luo, G. Li and D. Kessel, *Cancer Res.*, 1999, **59**, 3429–3432.
34 L. Y. Xue, S. M. Chiu and N. L. Oleinick, *Oncogene*, 2001, **20**, 3420–3427.
35 D. Kessel and A. S. Arroyo, *Photochem. Photobiol. Sci.*, 2007, **6**, 1290–1295.
36 F. Belloc, P. Dumain, M. R. Boisseau, C. Jalloustre, J. Reiffers, P. Bernard and F. Lacombe, *Cytometry*, 1994, **17**, 59–65.
37 M. C. DeRosa and J. Robert, *Coord. Chem. Rev.*, 2002, **233**, 351–357.
38 A. P. Castano, P. Mroz and M. R. Hamblin, *Nat. Rev. Cancer*, 2006, **6**, 535–545.
39 E. F. F. Silva, C. Serpa, J. M. Dabrowski, C. J. P. Monteiro, S. J. Formosinho, G. Stochel, K. Urbanska, S. Simoes, M. M. Pereira and L. G. Arnaut, *Chem.–Eur. J.*, 2010, **16**, 9273–9286.
40 Y. Vakrat-Haglili, L. Weiner, V. Brumfeld, A. Brandis, Y. Salomon, B. McIl-roy, B. C. Wilson, A. Pawlak, M. Rozanowska, T. Sarna and A. Scherz, *J. Am. Chem. Soc.*, 2005, **127**, 6487–6497.
41 M. E. Bulina, D. M. Chudakov, O. V. Britanova, Y. G. Yanushevich, D. B. Staroverov, T. V. Chepurnykh, E. M. Merzlyak, M. A. Shkrob, S. Lukyanov and K. A. Lukyanov, *Nat. Biotechnol.*, 2006, **24**, 95–99.
42 A. Roy, P. Carpentier, D. Bourgeois and M. Field, *Photochem. Photobiol. Sci.*, 2010, **9**, 1342–1350.
43 H. Ding, H. Yu, Y. Dong, R. Tian, G. Huang, D. A. Boothman, B. D. Sumer, J. Gao, B. D. Sumerb and J. Gao, *J. Controlled Release*, 2011, **156**, 276–280.
44 M. E. Milanesio, M. G. Alvarez, V. Rivarola, J. J. Silber and E. N. Durantini, *Photochem. Photobiol.*, 2005, **81**, 891–897.